Response reduction method for base-isolated buildings under long-period and long-duration ground motions

A. Kishida[(1)], K. Taga[(2)]

[(1)] Research Fellow, National Research Institute for Earth Science and Disaster Resilience, akiko_kishida@bosai.go.jp
[(2)] Professor, Kobe University, taga@tiger.kobe-u.ac.jp

Abstract

Recently, in Japan, earthquake ground motion that includes long-period components and persists for a long time (hereafter referred to a long-period and long-duration ground motion) has been recognized to negatively affect high-rise-buildings and base-isolated structures. The long-period and long-duration ground motion can cause excessive deformation in the isolation layer of the base-isolated building. Thus, the building can collide with the retaining walls if the clearance between them is insufficient. Moreover, the isolators and damping devices in the isolation layer may be ruptured. To prevent the occurrence of this phenomenon, it is possible to limit the response displacement of the isolation layer by adding a passive damper. Although this solution is effective during huge earthquakes, it can also increase the response acceleration during design earthquakes and lower the performance of the seismic isolation structure. In previous research, we developed a simply modified viscous damper called an on-off damper that can change the damping force depending on the response displacement and response velocity. The on-off damper reduces the damage to seismic-isolated structures undergoing excessive deformation during extreme earthquakes, without lowering the performance of the seismic-isolation system during earthquakes with medium to large magnitude. We have investigated the efficacy and effects of the proposed attenuator on the responses of a superstructure model under enormous pulse waves. However, investigations have not been conducted with regard to long-period and long-duration ground motion. In this study, we further investigated the effectiveness of the on-off damper in response to long-period and long-duration ground motion. We conducted an experiment using a shaking table and a test specimen that was a four-story model with a base isolation layer. An initial damper and two on-off dampers as supplemental dampers were installed on the base isolation layer. The input accelerations were the estimated long-period and long-duration earthquake ground motions, which were predicted to occur in the Osaka and Nagoya area in Japan for a huge earthquake occurring along the Nankai Trough (OS1 and CH1 earthquakes), and two level-2 observed earthquakes. To prevent ruptures of the base-isolation devices, we attached pneumatic cylinders as stoppers at both sides of the test specimen. In all cases of OS1 and CH1 long-period and long-duration ground motions, the specimen collided with the air cylinders. The test results revealed that the on-off dampers could reduce the responses compared with the results without the on-off dampers in the cases of the OS1 and CH1 ground motions. At the same time, in the cases of level-2 earthquakes, the on-off dampers could avoid lowering the performance of the seismic-isolation system by adjusting the initial clearance length to an appropriate value. Furthermore, we compare our analysis results with experimental results to review the effectiveness of the on-off damper from the analytical investigation. The numerical analysis results approximately agree with the test results for the long-period and long-duration ground motions.

Keywords: long-period ground motion, seismic-isolation structures, on-off dampers

1. Introduction

Recently, in Japan, earthquake ground motion that includes long-period components and persists for a long time (hereafter referred to a long-period and long-duration ground motion) has been recognized to negatively affect high-rise-buildings and base-isolated structures. In 2003, an earthquake occurred off the coast of Tokachi in Hokkaido. As a result, two tanks filled with petroleum and located approximately 250 km farther from the epicenter caught fire owing to sloshing. Thus, this problem became more noticeable. During the 2011 Tohoku Pacific Ocean earthquake, the skyscrapers in the Tokyo and Osaka bay area vibrated with a large amplitude. Tokyo and Osaka are located approximately 400 km and 800 km farther from the epicenter, respectively. It is considered that the main cause of these phenomena is the long-period and long-duration earthquake ground motion. Based on these events, in June of 2016, the Ministry of Land, Infrastructure, Transport, and Tourism provided technical advice for skyscrapers in the form of measures against the long-period ground motion caused by the extreme earthquake along the Nankai Trough [1].

The long-period and long-duration ground motion can cause excessive deformation in the isolation layer of the base-isolated building. Thus, the building can collide with the retaining walls if the clearance between them is insufficient. Moreover, the isolators and damping devices in the isolation layer may be ruptured. To prevent the occurrence of this phenomenon, it is possible to limit the response displacement of the isolation layer by adding a passive damper. Although this solution is effective during huge earthquakes, it can also increase the response acceleration during design earthquakes and lower the performance of the seismic isolation structure. In previous research, we developed an on-off damper that can change the damping force depending on the response displacement and response velocity [2-4] (Fig. 1). The on-off damper reduces the damage to seismic-isolated structures undergoing excessive deformation during extreme earthquakes, without lowering the performance of the seismic-isolation system during earthquakes with medium to large magnitude. We have investigated the efficacy and effects of the proposed attenuator on the responses of a superstructure model under enormous pulse waves. However, investigations have not been conducted with regard to long-period and long-duration ground motion. In this study, we further investigated the effectiveness of the on-off damper in response to long-period and long-duration ground motion. An experiment using a shaking table was conducted, and the test results were compared with the results obtained by numerical analysis.

Fig. 1 – On-off damper used in shaking table tests. Note the elongated hole in the damper joint, with the shown initial clearance length (*l*).

2. Shaking table test

2.1 Experimental contents

We conducted an experiment using a shaking table to confirm the effect of the on-off damper with regard to long-period and long-duration earthquake ground motions. The test specimen was a four-story model with a base isolation layer (Fig. 2), and its composition is presented in Table 1. Damping devices were installed onto the base isolation layer. We used a magnetorheological fluid (MR) damper as the initial damper. The force of the MR damper was controlled by changing the applied electric current. The MR damper was set to simulate the bilinear hysteresis of an oil damper with a valve relief, and the parameters are listed in Table 2. The additional dampers were on-off dampers with a damping coefficient of c=0.98 kN s/m. The initial clearance length (l) of the on-off dampers was adjusted in the 0-50 mm range, in increments of 10 mm. The oil damper in the on-off dampers had linear viscous damping force characteristics, and two on-off dampers were set in the base isolation layer. The combination of initial clearance lengths for two on-off dampers are denoted as (l_1, l_2) hereafter. The input accelerations were the estimated long-period and long-duration earthquake ground motions, which were predicted to occur in the Osaka and Nagoya area in Japan for a huge earthquake occurring along the Nankai Trough (OS1 and CH1 earthquakes [1]). Additionally, the two observed earthquakes (El Centro 1940 NS and JMA Kobe 1995 NS) were normalized to the maximum velocity of 50 cm/s (level-2 earthquakes). Figs. 3(a) and (b) show the time history waveforms of the input accelerations. Fig. 4 shows the velocity response spectrums of the OS1 and CH1 ground motions on the engineering bedrock for a damping factor of 5%. The OS1 and CH1 input waves were considered as the waves moving through the engineering bedrock, and were multiplied by 1.25 to consider the amplification by the surface ground. The similarity ratio of the length between the test and the real model was 1:4, and the time was condensed to half of the signal's original length. To prevent the rupture of the base-isolation devices, we attached moving control devices at both sides of the test specimen. A pneumatic cylinder with 1.25 kN and 2 kN of the ideal resultant output force represented the moving control device. The clearance between the test specimen and cylinder was set to 100 mm.

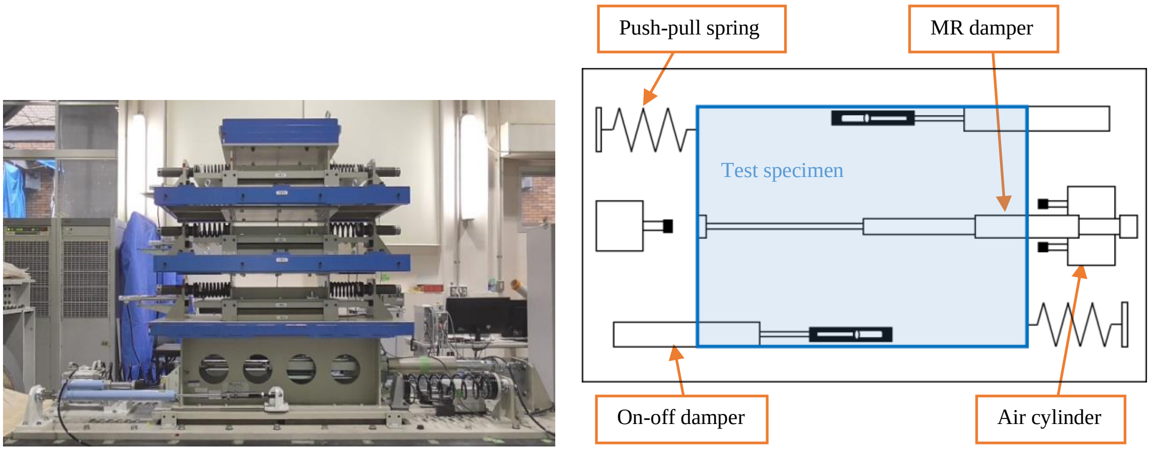

Fig. 2 – Experimental setup showing the four-story test structure (left) and setup plan (right).

Table 1 – Mass and stiffness parameters of four-storied test specimen.

STORY	MASS (kg)	STIFFNESS (kN/m)
4th	611.3	132.0
3rd	611.3	200.2
2nd	611.3	203.5
1st	713.2	22.7
First natural period of base isolation model: 2.36 (s)		
First natural period of fixed base model: 0.78 (s)		

Table 2 – Parameters of simulated bilinear hysteresis.

	UNIT	VALUE
Viscous damping coefficient (before relief)	kN/(m/s)	3.04
Post-relief viscous damping coefficient	kN/(m/s)	0.20
Relief force	kN	0.40
Velocity at relief	m/s	0.13
Maximum force	kN	0.57
Maximum velocity	m/s	1.00

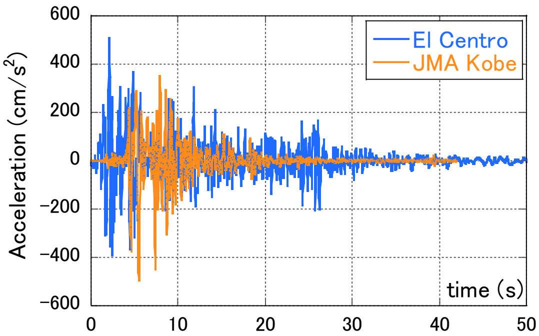

Fig. 3(a) – Time history waveforms of input accelerations from two observed earthquakes (1940 El Centro and 1995 JMA Kobe).

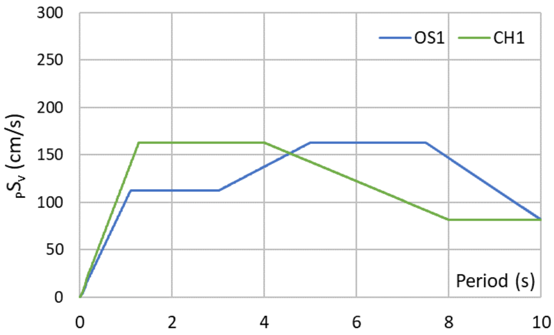

Fig. 4 – Velocity response spectrum of OS1 and CH1 ground motions on engineering bedrock for 5% damping factor.

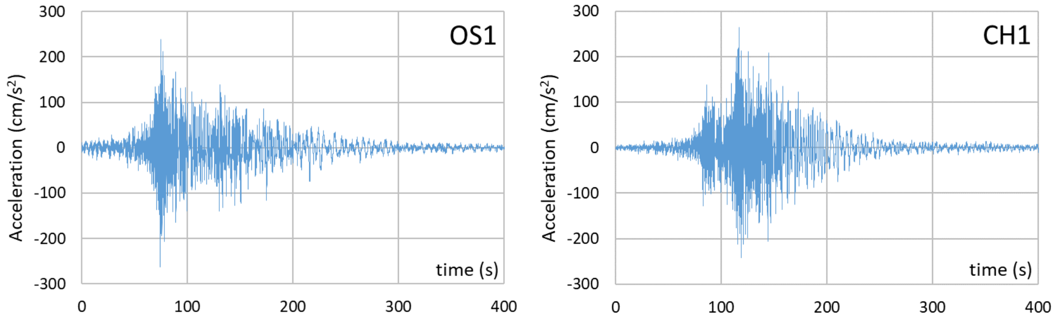

Fig. 3(b) – Time history waveforms of input accelerations from two estimated long-period and long-duration earthquake ground motions (OS1 and CH1 on engineering bedrock).

2.2 Test results

Figs. 5 and 6 show the maximum relative story displacement and maximum absolute acceleration, respectively, for each floor in response to the OS1 and CH1 ground motions, and 1.25 kN and 2 kN of the ideal resultant output force. The black solid lines indicate that the on-off dampers were not used, while the red solid lines indicate that conventional dampers were used (the initial clearance lengths were (l_1, l_2)=(0, 0)). The other lines indicate combinations of the initial clearance lengths, as shown in the legend. The results for each input type are shown. When the on-off dampers were added, all responses decreased compared with those without the on-off dampers. The on-off dampers with small initial clearance lengths tended to reduce the responses more effectively than those with large initial clearance lengths. In our experimental results, the conventional dampers did not cause the maximum reduction of the responses. For example, in the case of the maximum absolute acceleration responding to the OS1 ground motion, the (0, 10) and (0, 20) on-off dampers reduced the responses more than the conventional (0, 0) on-off dampers. This phenomenon does not pose a serious concern and is attributed to the differences between the input ground motions, test specimen-cylinders gaps, and resultant forces of the air cylinders, in all test cases.

Figs. 7 and 8 show the maximum relative story displacement and maximum absolute acceleration, respectively, for each floor, in response to the El Centro and JMA Kobe ground motions. In these cases, collisions with the air cylinders did not occur. When the conventional dampers were used as additional dampers, the absolute acceleration responses and inter-story drift of the upper structure increased. When the additional dampers changed to on-off dampers, in the case wherein the initial clearance lengths were small (for example, (10, 10)), the responses increased because the pin of the connection collided with the edge of the slot and the on-off dampers actuated. However, in the case wherein the initial clearance lengths were sufficiently large (for example, (30, 50)), there was approximately no change in the responses in comparison

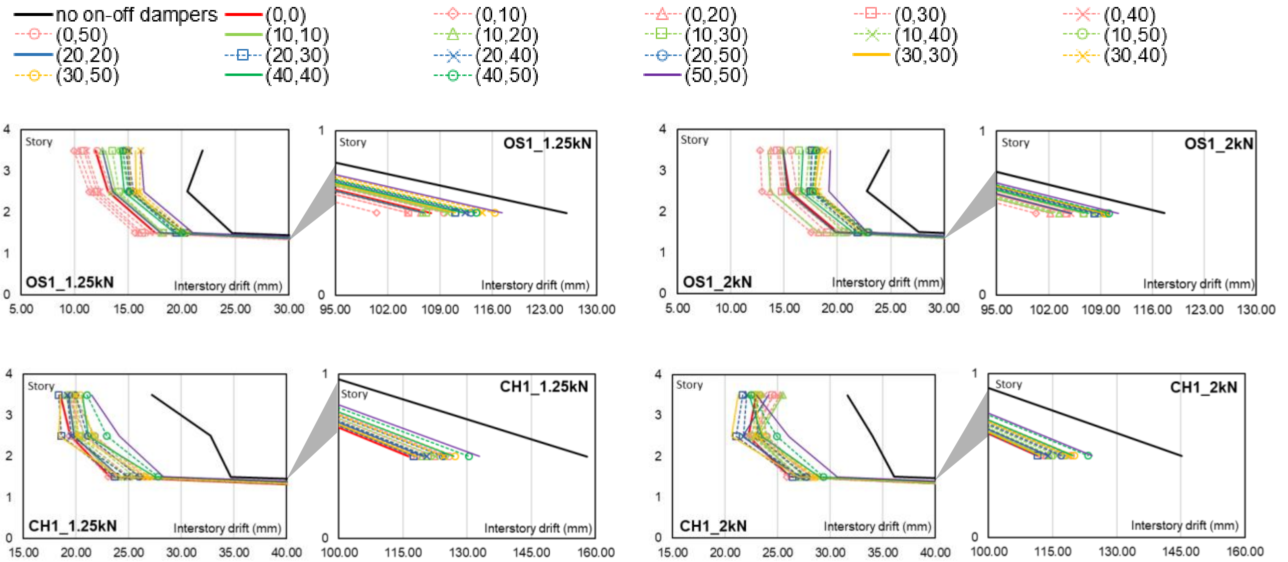

Fig. 5 – Maximum relative story displacement for each floor in response to OS1 and CH1 ground motions, and 1.25 kN and 2 kN of ideal resultant output force.

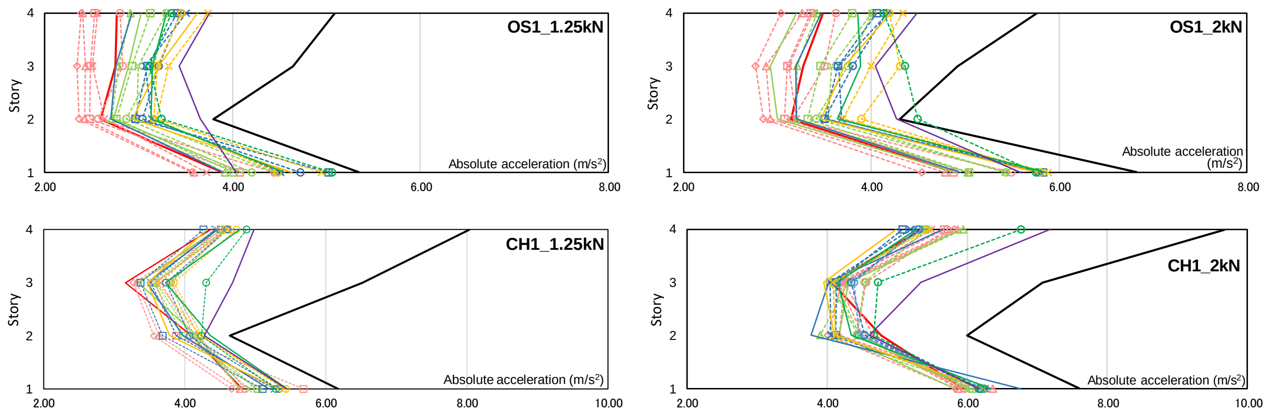

Fig. 6 – Maximum absolute acceleration for each floor in response to OS1 and CH1 ground motions, and 1.25 kN and 2 kN of ideal resultant output force.

with the case without on-off dampers. In response to the level-2 observed earthquake waves, the on-off dampers with sufficient initial clearance lengths did not damage the performance of the base-isolation system.

The results revealed that the on-off dampers could reduce the responses compared with the results without the on-off dampers in the cases of the OS1 and CH1 long-period and long-duration ground motions. At the same time, in the cases of level-2 earthquakes, the on-off dampers could avoid lowering the performance of the seismic-isolation system by adjusting the initial clearance length to an appropriate value. In a previous paper, we proposed a method of determining the appropriate lengths using optimization techniques [4].

3. Numerical Analysis

We compared the analytical results with the experimental results to review the effectiveness of the on-off damper from the analytical investigation. A four-mass shear model with a base-isolated story was provided, and the model parameters are listed in Table 2. A fixed damping factor of 3% was assumed for every story in

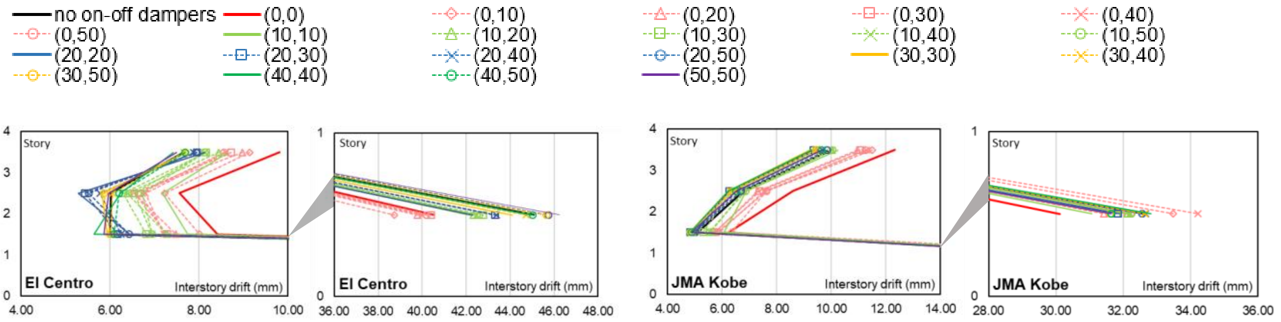

Fig. 7 – Maximum relative story displacement for each floor in response to level 2 observed earthquakes.

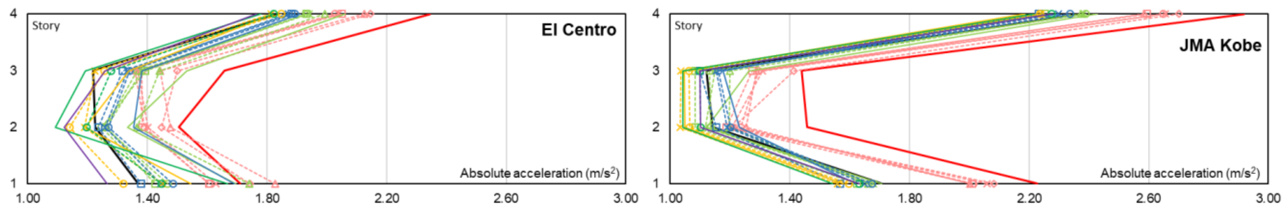

Fig. 8 – Maximum absolute acceleration for each floor in response to level 2 observed earthquakes.

the model. The damping devices installed at the base isolation layer are those described in Section 2. As the input acceleration, we used the acceleration that was actually measured in each shaking table test. For the level 2 observed earthquake, the numerical analysis results are in good agreement with the test results. In the case of the OS1 and CH1 ground motions, the specimen collided with the air cylinders several times. The clearances between the test specimen and cylinders were set as the displacement of the isolation layer at the time when the air cylinders started outputting in the collision case that the average value of resultant force for each cylinder becomed the maximum. In theory, the air cylinder is assumed to output a constant force. However, in practice, the resultant force is not constant. To represent the air cylinder in the numerical model, we used the maximum value of the average resultant forces, which were actually measured by the load cell at every collision as shown in Fig. 2.

Figs. 9(a) and (b) show the comparisons between the time history waveforms in the test results and those in the numerical analysis results, when an OS1 wave was input with the (10, 20) on-off dampers. Figs. 10(a) and (b) show the comparisons when an OS1 wave was input with the (30, 40) on-off dampers. Figs. 11(a) and (b) show the comparisons when an CH1 wave was input with the (10, 20) on-off dampers. Figs. 12(a) and (b) show the comparisons when an CH1 wave was input with the (30, 40) on-off dampers. In Figs. 9-12, (a) shows the waveforms of the relative story displacement for each inter-story, while (b) shows the waveforms of the absolute acceleration for each floor, when the ideal resultant force of the air cylinders was 1.25 kN. The relative story displacement waveforms of the test results agree with those of the analytical results. The absolute acceleration waveforms of the test results approximately agree with those of the analytical results, although the peak accelerations for the collisions with the air cylinders are not in good agreement. When one long-period and long-duration ground motion was input, the test specimen collided with the air cylinder several times. The test specimen-cylinder gaps and resultant forces of the air cylinders differed every time upon collision. However, in our analyses, they were set as constant during one input ground motion. This was considered as the cause of disagreement between the peak accelerations. Fig. 13 shows an enlarged graph for the time history waveforms of the test results and the results obtained by numerical analysis, when an CH1 wave was input with the (10, 50) on-off dampers and 2 kN air cylinders. As indicated by the red circles in Fig.13, when the collision with the air cylinder occurred in the experiment, it did not occur in the analysis. Additionally, when the collision occurred in the analysis, it did not occur in the experiment. Note that these results were obtained in some cases.

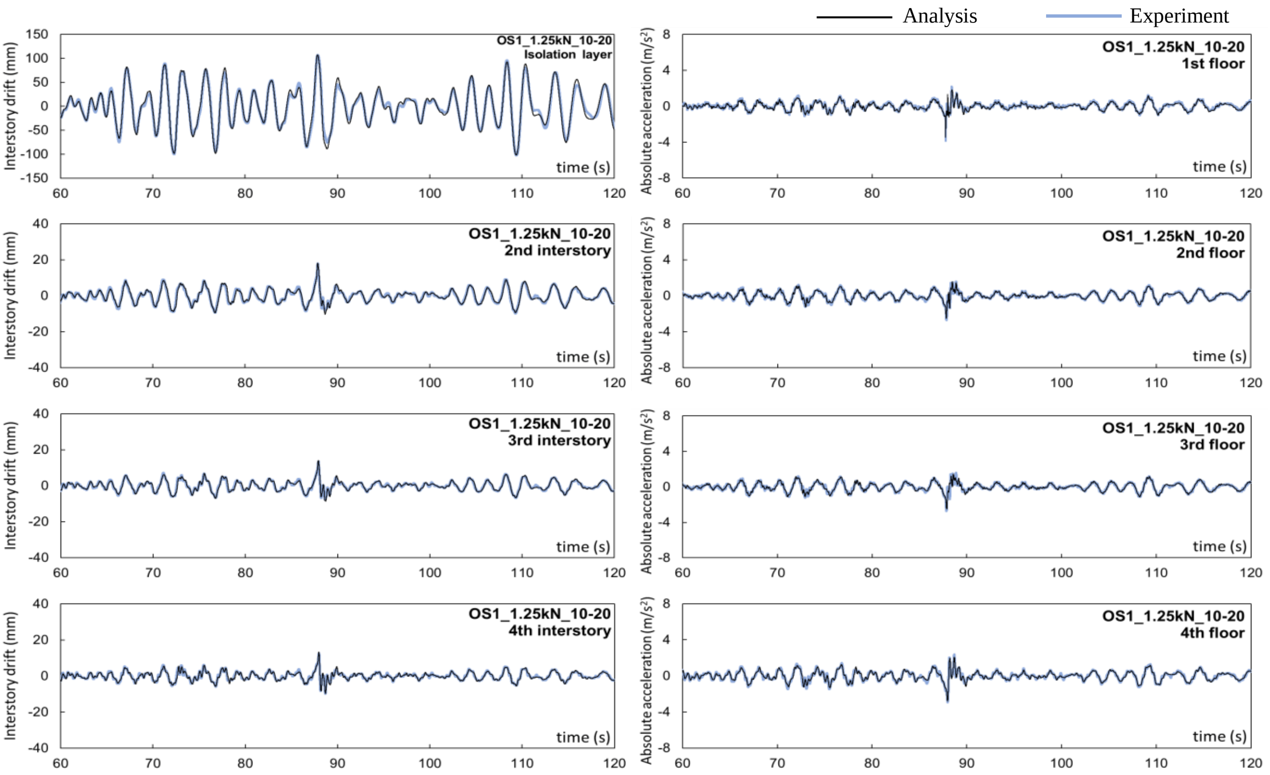

(a) Relative story displacement (b) Absolute acceleration

Fig. 9 – Time history waveforms of test results and numerical analysis results (OS1, (10, 20) initial clearance lengths, and 1.25 kN air cylinders).

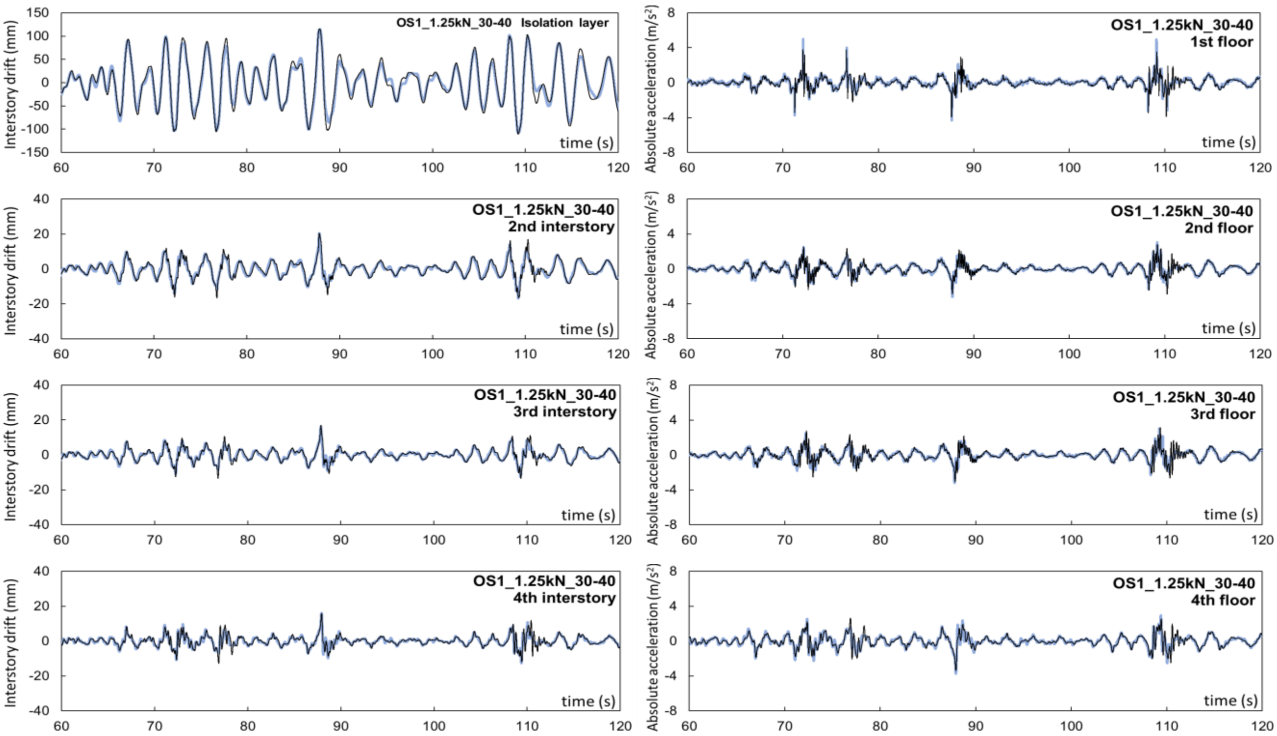

(a) Relative story displacement (b) Absolute acceleration

Fig. 10 – Time history waveforms of test results and numerical analysis results (OS1, (30, 40) initial clearance lengths, and 1.25 kN air cylinders).

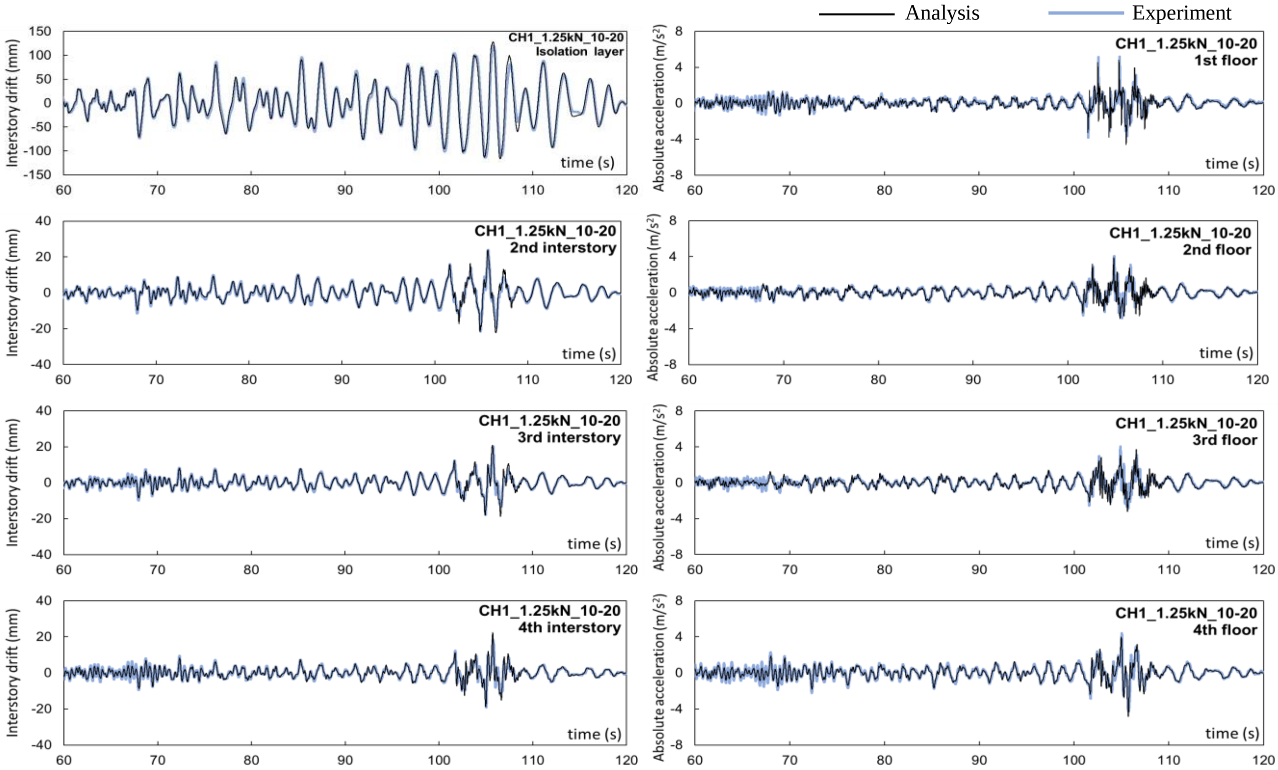

(a) Relative story displacement (b) Absolute acceleration

Fig. 11 – Time history waveforms of test results and numerical analysis results (CH1, (10, 20) initial clearance lengths, and 1.25 kN air cylinders).

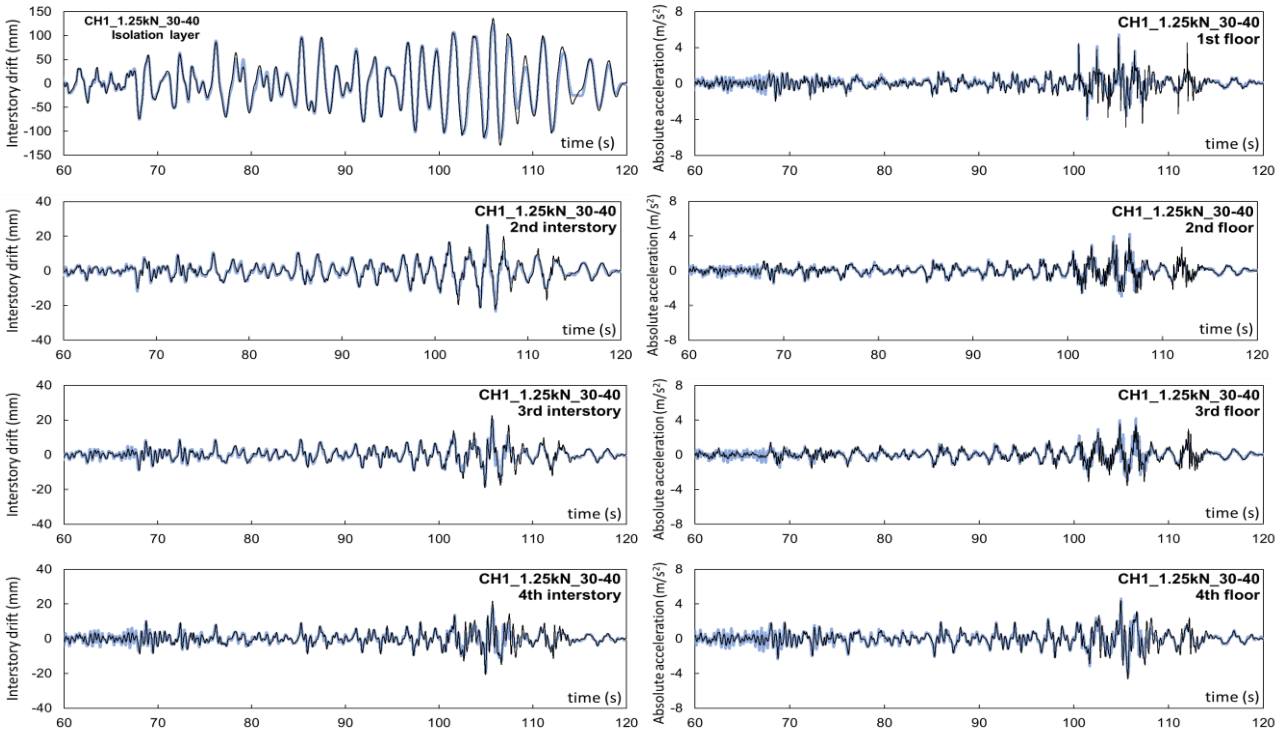

(a) Relative story displacement (b) Absolute acceleration

Fig. 12 – Time history waveforms of test results and numerical analysis results (CH1, (30, 40) initial clearance lengths, and 1.25 kN air cylinders).

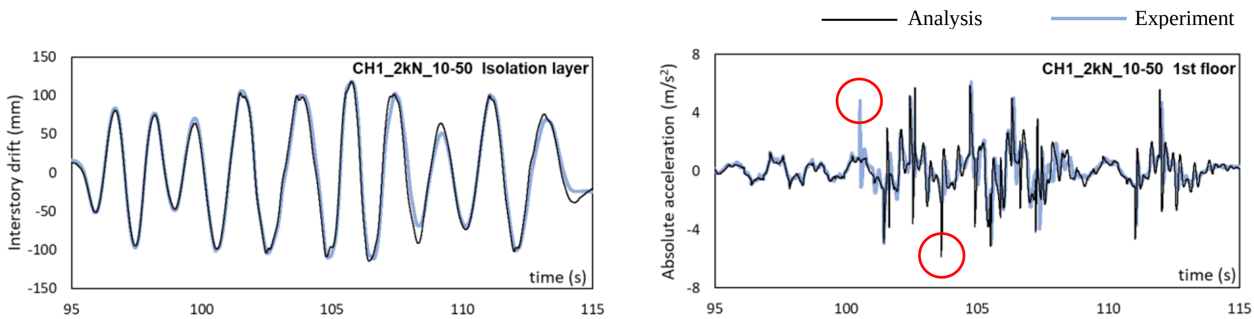

Fig. 13 – Enlarged graph of time history waveforms obtained by test results and numerical analysis results for absolute acceleration (CH1, (10, 50) initial clearance lengths, and 2 kN air cylinders).

Table 3 shows the numbering for all combinations of initial clearance lengths. Fig. 14 shows the ratios of the analytical maximum response divided by the test results for the absolute acceleration and relative story displacement responses, respectively, to OS1, for each floor and all initial clearance combination cases, with the 1.25 kN air cylinder. Fig.15 shows the ratios to OS1 with the 2 kN air cylinder. Fig. 16 shows the ratios to CH1 with the 1.25 kN air cylinder. Fig.17 shows the ratios to CH1 with the 2 kN air cylinder. The ratios for the relative story displacement were approximately equal to 1, except for the case without the on-off dampers and the ratios of the 3rd and 4th inter-story for CH1 ranging within an error of approximately 20%. The ratios for the absolute acceleration ranged within an error of approximately 10%, except in the case without the on-off dampers wherein the collisions with the air cylinders were more intense compared with those in the cases with the on-off dampers. Then, the differences in the conditions of the test specimen-cylinder gaps and the resultant forces of the air cylinders were larger between the analytical and experimental results. Thus, we assumed that this was the reason for the analysis results not being able to trace the test results in the cases without the on-off dampers.

Table 3 – Numbering for combinations of initial clearance lengths (l_1, l_2) (mm)

No.	(l_1, l_2)	No.	(l_1, l_2)	No.	(l_1, l_2)	No.	(l_1, l_2)	No.	(l_1, l_2)	No.	(l_1, l_2)
1	(0,0)	5	(0,40)	9	(10,30)	13	(20,30)	17	(30,40)	21	(50,50)
2	(0,10)	6	(0,50)	10	(10,40)	14	(20,40)	18	(30,50)		
3	(0,20)	7	(10,10)	11	(10,50)	15	(20,50)	19	(40,40)		
4	(0,30)	8	(10,20)	12	(20,20)	16	(30,30)	20	(40,50)		

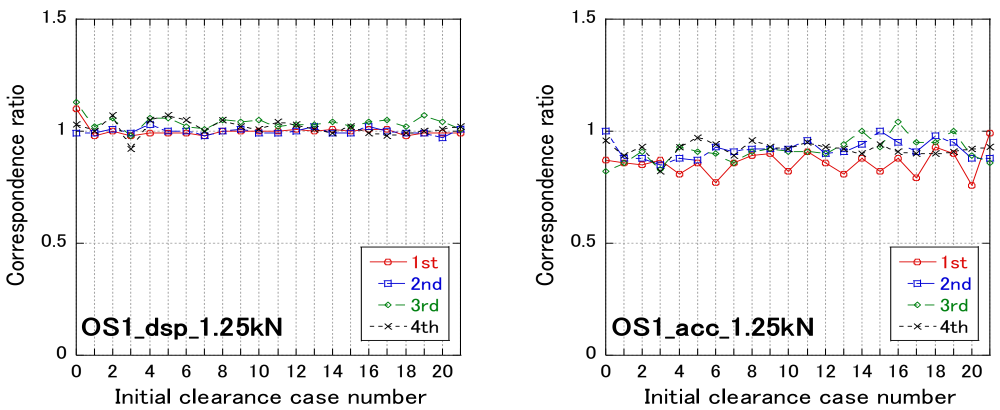

Fig. 14 – Ratios of analytical maximum response divided by test results for relative story displacement (left panel) and absolute acceleration (right panel) responses, respectively, to OS1, for each floor and all initial clearance combination cases, with 1.25 kN air cylinder.

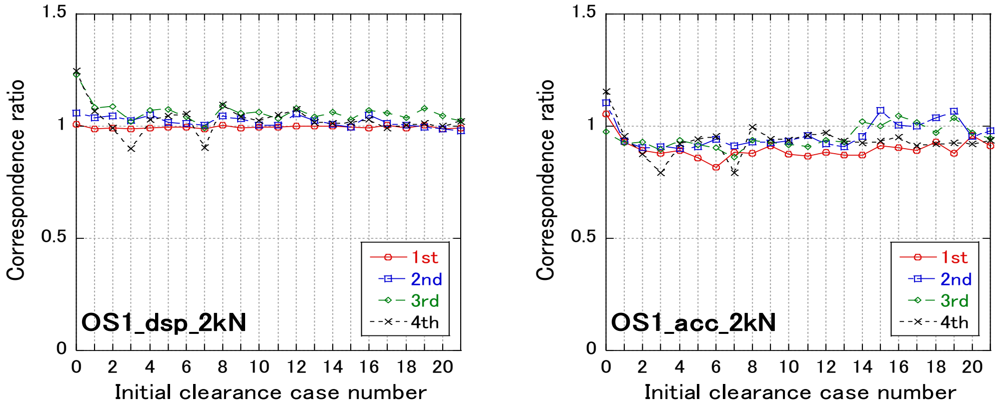

Fig. 15 – Ratios of analytical maximum response divided by test results for relative story displacement (left panel) and absolute acceleration (right panel) responses, respectively, to OS1, for each floor and all initial clearance combination cases, with 2 kN air cylinder.

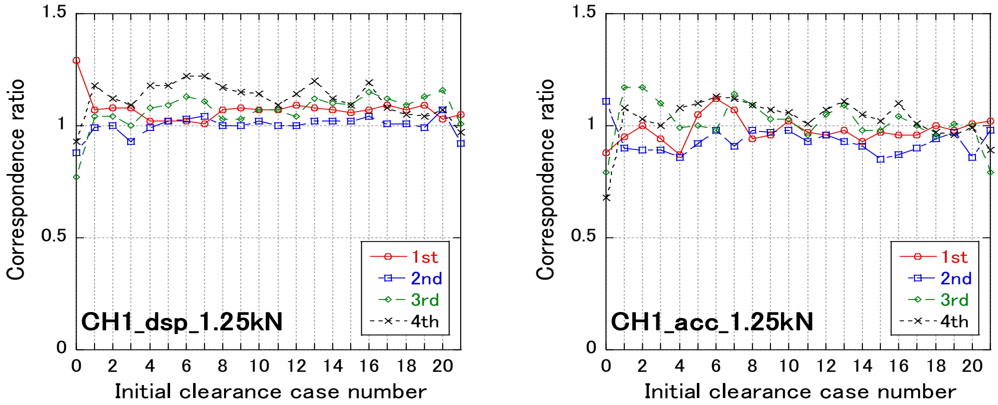

Fig. 16 – Ratios of analytical maximum response divided by test results for relative story displacement (left panel) and absolute acceleration (right panel) responses, respectively, to CH1, for each floor and all initial clearance combination cases, with 1.25 kN air cylinder.

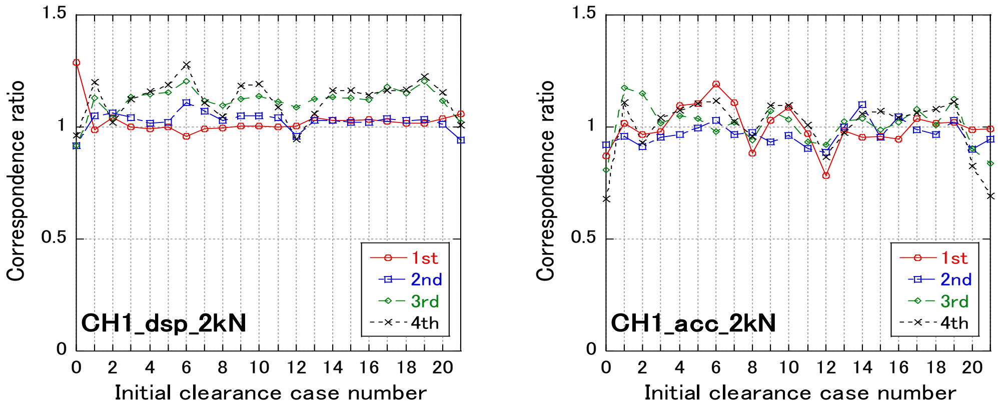

Fig. 17 – Ratios of analytical maximum response divided by test results for relative story displacement (left panel) and absolute acceleration (right panel) responses, respectively, to CH1, for each floor and all initial clearance combination cases, with 2 kN air cylinder.

4. Conclusion

1) We conducted a shaking table test and numerical analyses to investigate the efficacy and effects of the proposed on-off damper in response to long-period and long-duration ground motions.

2) The experimental results confirmed that the on-off dampers could reduce the absolute acceleration and relative story displacement responses in the cases of OS1 and CH1 ground motions. Moreover, in the cases of level-2 earthquakes, the on-off dampers could avoid the diminished performance of the seismic-isolation system by adjusting the initial clearance length.

3) The numerical analysis results approximately agree with the test results for the long-period and long-duration ground motions. Thus, it is concluded that the disagreement between the analytical and test results was caused by the differences of the test specimen-cylinder gaps and the differences in the resultant forces of the air cylinders.

5. Acknowledgements

This study was supported by The Keihanshin Consortium for Fostering the Next Generation of Global Leaders in Research (K-CONNEX), established by the Human Resource Development Program for Science and Technology, MEXT.

6. References

[1] Building Research Institute (2002): Technical data for countermeasure against long-period ground motions. https://www.kenken.go.jp/japanese/contents/topics/lpe/index.html (in Japanese)

[2] Kishida A, Nishimura N, Yamashita Y, Taga K, Fujitani H, Mukai Y (2017): Response reduction methods for base isolated buildings with collision to retaining walls. *SPIE 10168, Sensors and Smart Structures Technologies for Civil, Mechanical, and Aerospace Systems (1016810)*, Portland, OR.

[3] Kishida A, Yamashita Y, Nishimura N, Taga K (2017): Response reduction methods for base-isolated buildings that collide with retaining walls -Influence of initial clearance length. *The 12th Japan-China Joint Conference on Structural Engineering (309)*, Kobe, Japan.

[4] Kishida A, Yamashita Y, Ueda U, Taga K (2018): Optimization of on-off dampers for reducing collision of base-isolated buildings with retaining walls. *The 11th National Conference in Earthquake Engineering*, Earthquake Engineering Research Institute, (ID 1227), Los Angeles, CA.

